Kinetic and thermodynamic studies on the adsorption of Cu^{2+} ions from aqueous solution by using agricultural waste-derived biochars

Nihan Kaya, Ferhat Arslan, Zeynep Yıldız Uzun and Selim Ceylan

ABSTRACT

In this study, it was aimed to investigate the adsorption properties of the biochars obtained by pyrolysis of hazelnut and walnut shells for removal of copper ions from aqueous solutions. The characterization of raw biomasses and also biochars were performed using TGA-DTG, FT-IR, BET, SEM, partial and elemental analysis techniques. The optimum conditions were determined by investigating the effect of adsorption parameters (initial concentration, temperature, adsorbent amount, pH, contact time and mixing speed) for efficient removal of copper ions from aqueous solution by batch adsorption experiments carried out under different conditions. The highest adsorption efficiencies were recorded as 82 and 86% respectively for hazelnut and walnut shell biochars at pH 4, $C_o = 15$ ppm, adsorbent dosage = 3 g/L and mixing speed = 600 rpm. Experimental results showed that the adsorption efficiency for copper ions increased with the increase of temperature (T = 45 °C) in studies only using biochar obtained from hazelnut shell. While the time of equilibrium in the aqueous solution containing copper ions was determined to be 75 min for walnut shell char, this duration was 30 min for hazelnut shell char. The experimental results were investigated in terms of Langmuir, Freundlich and Temkin isotherm models. Together with the calculated thermodynamic parameters, the adsorption mechanism was explained. In order to determine the kinetic model of the adsorption process, the experimental data were applied to pseudo first-order, pseudo second-order and intra-particle diffusion models, and the model constants were investigated.

Key words | adsorption, biochar, copper ions, hazelnut shell, pyrolysis, walnut shell

Nihan Kaya (corresponding author)
Ferhat Arslan
Faculty of Engineering, Chemical Engineering Department,
Hitit University,
Çorum,
Turkey
E-mail: *nihankaya@hitit.edu.tr*

Zeynep Yıldız Uzun
Boyabat Vocational School, Department of Chemistry and Chemical Processing Technologies,
Sinop University,
Sinop,
Turkey

Selim Ceylan
Faculty of Engineering, Chemical Engineering Department,
Ondokuz Mayıs University,
Samsun,
Turkey

HIGHLIGHTS

- Agricultural wastes are promising candidates for wastewater treatment.
- Copper removal from aqueous solution by using biochars is a most attractive and low cost treatment option compared with commercially available activated carbon.
- The option offers environmental and socio-economic advantages and sustainability.

INTRODUCTION

One of the most important reason for water pollution is undoubtedly industrial wastewater containing heavy metals. These materials, which can be harmful even in trace amounts and are considered systemic toxicants, include elements such as lead, zinc, copper, cobalt, cadmium, chromium, nickel, arsenic, mercury, silver etc (Tchounwou *et al.* 2012). Copper pollution in water resources is especially caused by copper mines, smelting operations, electro-plating, metal-finishing and paint industries (Karabelli *et al.* 2011; Ghrab *et al.* 2017). It is of great importance that

doi: 10.2166/ws.2020.193

copper, widely used in industry due to its superior physical and chemical properties, is removed from water sources using appropriate techniques.

Conventional methods for removing heavy metal pollution from wastewater include chemical precipitation, chemical oxidation/reduction, chemical coagulation, ion-exchange, electrochemical methods, membrane processes and ultrafiltration. However, these techniques have some limitations such as high operating cost, low efficiency, sensitive operating conditions, and the production of secondary sludge (Alalwan *et al.* 2020). Therefore, in recent years, scientists have conducted various researches in order to develop easy, low cost and environmentally friendly techniques which can obtain the maximum analytical yield in water treatment. One of these techniques is adsorption, which is a highly efficient advanced treatment method for the removal of pollutants that is particularly stable for conventional methods (Gaouar-Yadi *et al.* 2016). In this purification technique, the rate and amount of adsorption is a function of the adsorbent surface. For this reason, materials with high surface area are used as an adsorbent. Especially, the high adsorption capacity, high active surface area and microporous structure make activated carbon the most suitable adsorbent (Demiral & Aydın Şamdan 2016). However, the high price of commercial activated carbon has effected the search for cheaper new adsorbents with similar properties. There have been many studies in the literature on active carbon production using carbon-containing agricultural by-products and wastes and their usability as alternative adsorbents in water treatment. Different biomasses (precursors) such as pine cone (Dawood *et al.* 2017), saffron leaves (Dowlatshahi *et al.* 2014), sugarcane bagasse (Gonçalves *et al.* 2016), peach stones (Masiya & Gudyanga 2009), waste tea (Shen *et al.* 2016), waste cherry kernels (Vukelic *et al.* 2018), apricot shell (Yi *et al.* 2013) and so on have been used in the production of active carbon.

In literature, numerous investigations have been conducted into the utilization of waste agricultural materials to remove copper ions from wastewater. However, in most of these studies, removal efficiency has been reported for raw biomass used as adsorbent such as wheat bran (Wang *et al.* 2009), orange peel (Sha *et al.* 2009), mango peel (Iqbal *et al.* 2009), pomegranate peel (Ben-Ali *et al.* 2017), banana peel (Ince *et al.* 2017), peanut hull (Zhu *et al.* 2009), chestnut shell (Ince *et al.* 2017), tea waste (Amarasinghe & Williams 2007) and garden grass (Hossain *et al.* 2012) etc. In recent years, these raw biomasses, which have been the focus of interest since the 1990s, have been carbonized to produce biochars at different pyrolytic temperatures and have been used to adsorb copper ions from contaminated water. While recent limited studies have reported adsorption capacity of Cu(II) ions onto biochars produced from various local sources such as molasses, olive branches etc. (Legrouri *et al.* 2017; Fazal-ur-Rehman 2018; Alkherraz *et al.* 2020), there are not enough studies to fully explain the adsorption mechanisms of copper ions on biochars especially derived from hazelnut and walnut shells. Whereas, in many countries producing hazelnuts and walnuts all over the world, tons of crust are emerging every year as waste. These waste materials are of limited use and are either used as fuel or directly pollute the environment. For this reason, conversion of agricultural wastes such as hazelnut and walnut shells into biochars is of great importance in order to prevent environmental pollution. It can also contribute to the economy by converting these natural resources efficiently into high value-added products.

The aim of this study is to determine the adsorption properties of biochars produced by pyrolysis of hazelnut and walnut shells for removal of copper ions from aqueous solutions. For this purpose, firstly both biomass and biochar characterization studies were carried out by determining their chemical, thermal and surface properties. Then, batch adsorption experiments were carried out as a function of the initial heavy metal concentration, temperature, adsorbent amount, pH, contact time and mixing speed. Finally, the equilibrium, kinetics and thermodynamics of Cu^{2+} adsorption onto biochars were investigated.

MATERIALS AND METHODS

Materials

In this study, hazelnut and walnut shell biomass, an agricultural waste, were collected from Ordu and Samsun provinces in Turkey respectively. The samples were dried at 70 °C for 12 h (Uniterm, mst 55). The dried sample was

reduced in size by passing it through a stainless steel blade mill (Waring, USA). Samples were sieved and those with dimensions less than 250 μm were used in experiments. Thus, heat and mass transfer limitations were prevented.

Experimental solutions used in the batch adsorption experiments was prepared with the help of standard copper nitrate ($Cu(NO_3)_2$) solution obtained from Merck.

Characterization of raw materials

Proximate and ultimate analysis

Proximate analysis of the samples was carried out using an ash furnace (Protherm, PLF120/5). For the volatile matter determination, 1.00 g of hazelnut and walnut shell samples were taken into the crucible and placed in an ash furnace at 950 ± 5 °C for 8–10 min. The crucible was then cooled and weighed. For ash analysis of the samples, 1.00 g of sample was taken into the crucible and placed in an ash furnace at 800 °C for 60 min. The cooled crucible was weighed and the amount of ash calculated. To determine the moisture content of the biomass, 1.00 g of hazelnut and walnut shell samples were placed in a crucible and the sample was heated at 70 °C for 24 h. At the end of the process, the cooled crucible was weighed and the amount of moisture was calculated.

Ultimate analysis of raw hazelnut and walnut shell was performed on a Leco brand CHNS-932 model analyzer. Quantities of C, N, H and S were measured simultaneously.

TGA-DTG analysis

The thermal behaviors of hazelnut and walnut shells were determined in a thermogravimetric analyzer (TA, DMAQ800). Approximately 10 mg of sample was placed in the alumina pan and loaded into the device. Experiments were carried out under an inert nitrogen atmosphere using a gas flow rate of 80 mL/min. The temperature was then increased to 800 °C at a heating rate of 10 °C/min and the mass losses of the samples were recorded on the computer as a function of temperature and time.

FT-IR analysis

FT-IR spectra of raw hazelnut and walnut shells were recorded using a Perkin Elmer (USA) brand FT-IR spectrometer between 400 cm^{-1} and 4,000 cm^{-1} by pellets made with KBr. In the obtained spectra, the structures of the biomasses were defined with the help of the peaks given by the surface functional groups.

Preparation of biochar (pyrolysis experiment)

Pyrolysis of hazelnut and walnut shell biomass was carried out at different temperatures in the temperature range of 400–700 °C using a 20 g sample in an electrically heated fixed bed pyrolysis reactor with a volume of 600 cm^3. During the process, the inert nitrogen gas flow rate was set to 100 mL/min and the heating rate to 20 °C/min. The reactor temperature was supplied by the heat-couple placed inside the reactor from the top of the furnace. After the pyrolysis temperature reached the desired values, it was held at the desired temperature for 60 min, so that the pyrolysis process was completed.

Characterization of the biochars

BET analysis

The BET surface area was obtained from nitrogen adsorption isotherms at 77 K by using a Quantachrome/IQ-Chemi surface area analyzer. Prior to gas adsorption measurement, the sample was degassed at 200 °C under vacuum for 12 h. The adsorption data were obtained in a relative pressure. The BET surface area was calculated from N_2 adsorption isotherms by using the Brunauer-Emmett-Teller (BET) equation.

SEM analysis

To clarify the surface properties and morphology of the biochar samples before and after heavy metal adsorption, topographic images of the sample surface were taken with the Quanta (USA) FEI/Quanta 450 FEG brand SEM device and structural changes were determined.

Batch adsorption experiments

In this study, in order to determine the removal efficiency of Cu(II) ions from aqueous solution, batch adsorption experiments were carried out. Commercially available stock solution with a concentration of 1,000 mg/L were diluted with distilled water to the desired concentration to prepare the test solutions to be used in the adsorption experiments. Batch equilibrium adsorption studies were performed using 250 mL of heavy metal solution. Parameters affecting the adsorption process such as pH (2.5–5), adsorbent dosage (1–3 g/L), initial heavy metal concentration (15–45 ppm), contact time (up to 300 min), temperature (25–45 °C) and mixing speed (200–600 rpm) were studied in a batch system. pH of the solutions was adjusted by 0.1 M HCl and 10% (w/v) NH_3 solutions. The samples were collected at predetermined time intervals and the adsorbent separated from the samples by filtering. The filtrate was analyzed by ICP-OES (Perkin Elmer, Optima 5300 DV) to determine the residual Cu(II) ion concentration. Based on the acquired values, the amount of heavy metal ion adsorbed per unit mass of the adsorbent (q_e) was calculated according to Equation (1) and the adsorption yield was calculated by using Equation (2). As a result, optimum removal conditions of copper ions were determined.

$$q_e = (C_0 - C_e) \times \frac{V}{m} \quad (1)$$

$$Heavy\ \ Metal\ \ Removal(\%) = \frac{C_0 - C_e}{C_0} \times 100 \quad (2)$$

where q_e is the amount of adsorbed copper ions per gram of adsorbent (mg/g), C_o and C_e are the initial and final copper concentration in the solution phase, respectively (ppm), V is the volume of copper solution (L) and m is the weight of adsorbent (g). In order to ensure the reproducibility of the results, all the adsorption experiments were performed in triplicate and the average values were used in data analysis. Relative standard deviations were found to be within ±1%.

RESULTS AND DISCUSSION

Characterisation of hazelnut and walnut shell

Hazelnut and walnut shell samples were characterized together with proximate and ultimate analysis, and the results are presented in Table 1. Hazelnut and walnut shell biomass have different properties due to their differences in composition. Biomass with less than 10% moisture content is considered the best feedstock for pyrolysis and combustion (Balasundram *et al.* 2017; Muhammad *et al.* 2017). Although the moisture content (2.83%) of hazelnut shells used in our studies is slightly higher than that of walnut shells (2.18%), it has potential to be used as feedstock in the pyrolysis process because of having a moisture content lower than 10% for both raw materials. Another important parameter affecting the pyrolysis process is the volatile matter content in the biomass. High amounts of volatile substances in the raw material are more concentrated in the pyrolysis oil, which is one of the products that are generally released during the pyrolysis process. According to the literature, volatile matter content in different biomass samples subjected to pyrolysis varies between 48 and 87% (Saidur *et al.* 2011). When we compared both raw materials according to the literature, it was seen that they have high volatile matter content. The proportion of volatile components in the hazelnut shell used in our studies (81.39%) was higher than that of the walnut shell (74%).

Table 1 | Proximate and ultimate analysis of walnut and hazelnut shell

Proximate analysis (wt.%)	Walnut shell	Hazelnut shell
Moisture	2.18	2.83
Volatile matter	74.00	81.39
Ash	5.00	1.32
Fixed carbon[a]	18.82	14.46
Ultimate analysis (wt.%)	**Walnut shell**	**Hazelnut shell**
C	45.32	47.77
H	5.54	5.82
N	1.12	1.09
S	1.85	1.67
O[a]	46.17	43.65

[a]By difference.

The high volatiles that both raw materials have, in the pyrolysis process, will drift away from the environment due to the effect of temperature and the fixed carbon, the main component of the biochar, will remain. The amount of ash, one of the inorganic components in the biomass structure, was found to be 1.32 and 5% for hazelnut and walnut shells, respectively. The amount of ash in the hazelnut shell was considerably lower than that of the walnut shell. In the literature, the ash content of different biomass samples varied between 0.1 and 38% (Soyler *et al.* 2017). The low ash content of both raw materials compared to the literature suggests that they may be a good starting material for the preparation of carbon-based biochar to be used as adsorbents (Jian *et al.* 2018).

According to the elemental analysis results in Table 1, S and N compositions of hazelnut and walnut shells were found to be 1.67%, 1.09% and 1.85%, 1.12% respectively. It is very important that the S and N values in the biomass are low, because both components are elements that can cause environmental problems and also corrosion in the pyrolysis reactor.

The thermogravimetric analysis (TG) and differential thermogravimetric analysis (DTG) curves of raw biomass were used to determine the mass loss steps to occur during pyrolysis of the walnut and hazelnut shell samples used in the study. In Figure 1, the TG and DTG curves for the raw materials obtained at a heating rate of 10 °C/min are given. The first stage in the TG curves is the preheating stage from ambient temperature to 180 °C. Because of the water and volatile compounds removed from the hazelnut and walnut shells, mass losses were 5.81% and 3.84%, respectively at this stage. Hazelnut and walnut shells mainly consist of hemicellulose, cellulose and lignin like all other lignocellulosic materials (Uzun & Yaman 2017). The decomposition of hemicellulose and cellulose, which are the main constituents of biomass, occurs at temperatures between 120 °C and 350 °C (Ghaffar & Fan 2013). When TG curves were examined, it was determined that hemicellulose and cellulose in hazelnut and walnut shells were separated from the structure at 233–337 °C and 198–295 °C respectively in the second stage. The decomposition of hemicellulose and cellulose occurred at higher temperature in the hazelnut shell. In the third stage, the decomposition of lignin, the most resistant component of hazelnut and walnut shells, occurred at temperatures between 342–397 °C and 307–383 °C, respectively. DTG curves show that all lignocellulosic compounds (cellulose, hemicellulose and lignin) in the structure of hazelnut and walnut shells are separated from the structure at temperatures between 233–397 °C and 198–383 °C, respectively. In the meantime, mass loss was observed to be 62.82% and 49.53%, respectively. The results of thermogravimetric analyses carried out for the characterization of raw biomass have been concluded to be consistent with the decomposition curves of woody-cellulosic biomasses such as hazelnut and walnut shells previously reported in the literature (Uzun & Yaman 2017; Xu *et al.* 2017).

The FT-IR spectrum of raw hazelnut and walnut shell is given in Figure 2. When the FT-IR spectra were examined, wide vibration bands observed around the 3,334 cm^{-1} and 3,393 cm^{-1} wavelength indicated the presence of hydroxyl (-OH) groups originating from the water molecule in the structure that were more intense in the hazelnut shell. According to the results of the proximate analysis, the moisture content of the hazelnut shell was higher than that of the walnut shell, and this result supported the fact that the O-H stretching vibration in the hazelnut shell spectrum was more severe than the walnut shell. The C-H stretching vibration observed between 2,934 and 2,887 cm^{-1} for both biomass indicated the presence of aliphatic hydrocarbons. Asymmetric stretching vibrations in the FT-IR spectrum of both hazelnut and walnut shells at around 1,618–1,741 cm^{-1} belonged to C = O stretching and showed the presence of functional groups of acid, aldehyde and ketone compounds in the structure. The C = O stretching vibration was observed as a more severe and sharp peak in the hazelnut shell. The existence of aliphatic groups was understood from C-H vibrations observed at around 1,460 cm^{-1}. It could be said that the C-O and C-O-H stretching vibrations observed at around 1,200 cm^{-1} belonged to compounds such as ether, alcohol and phenol in the structure (Liu *et al.* 2015; Odeh 2015; Plis *et al.* 2015; Niu *et al.* 2016). Similar FT-IR spectrums were also obtained in bio-chars derived from hazelnut and walnut shells. According to these spectrums, the distributions of functional groups on the bio-char surface were the same as the raw biomass. Especially, the functional groups such as carboxyl and hydroxyl groups on the biochar surface may have played

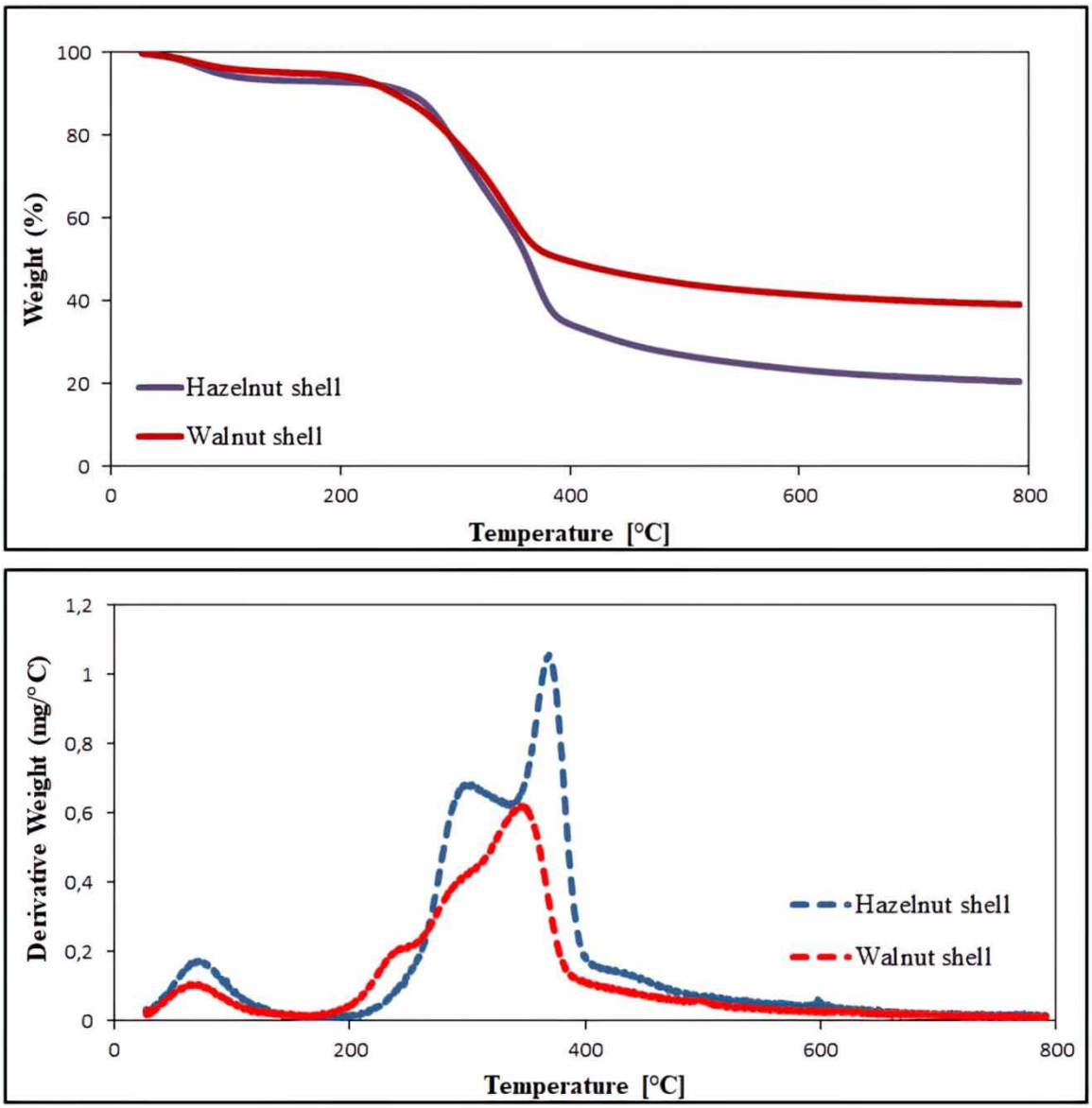

Figure 1 | TG-DTG curves of hazelnut and walnut shell at heating rate of 10 °C/min.

an important role in binding copper ions onto the biochar surface (Park *et al.* 2017).

Characteristics of biochars

The quality and physicochemical properties of biochar obtained by pyrolysis of biomass are dependent on the physical and chemical properties of the raw material that is used in the process and the pyrolysis conditions (Kim *et al.* 2001). Since the carbonization temperature changes the surface area of the biochar and consequently the adsorption capacity, it is one of the most important parameters. Generally, surface area increases with pyrolysis temperature increase due to the escape of volatiles during carbonization (Park *et al.* 2017). In this study, pyrolysis was carried out separately at different carbonization temperatures in the range of 400–700 °C under 100 mL/min nitrogen flow. Specific surface areas of biochar obtained by carbonization of

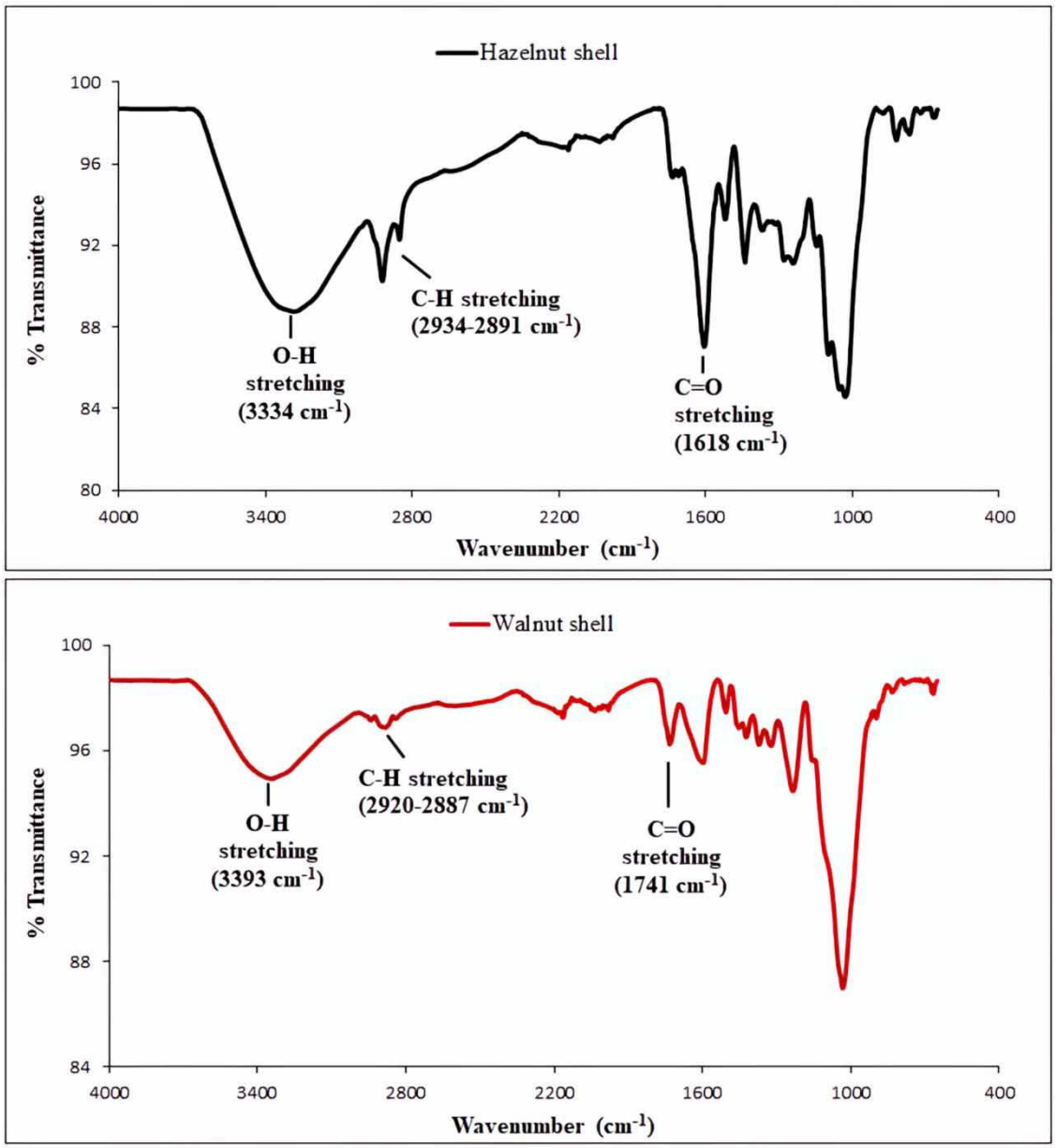

Figure 2 | FT-IR spectrum of raw walnut and hazelnut shell.

hazelnut and walnut shells at different temperatures were determined by BET method. The effect of the pyrolysis temperature on the BET surface area is given in Figure 3.

As can be seen in Figure 3, the surface area of biochar produced from hazelnut shell increased from 5.579 m^2/g to 124.347 m^2/g with an increase in carbonization temperature between 400 and 500 °C, and then decreased to 81.541 m^2/g at 600 °C. As the temperature rises to 500 °C, some compounds resulting from cross-linking reactions caused the surface area to increase. After this point, due to the collapse of the carbon structures that were formed with increasing temperature, a decrease in surface area was observed (Demiral & Aydın Şamdan 2016). As a result, the high temperature had an adverse effect on the surface area of the biochar obtained from hazelnut shell and the highest BET

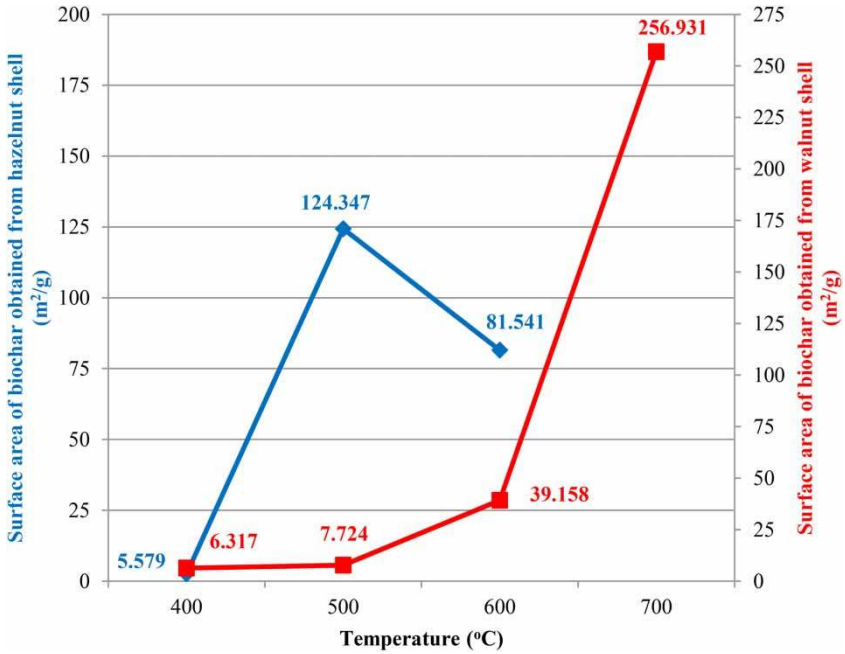

Figure 3 | BET surface area values of biochar samples obtained from hazelnut and walnut shells at different pyrolysis temperatures.

surface area value was reached at 500 °C. On the contrary, the high temperature had a favorable effect on the surface area of the biochar obtained from walnut shell and the surface area increased considerably by increasing the pyrolysis temperature from 400 °C to 700 °C. In particular, the maximum surface area value (256.931 m^2/g) was achieved with increasing temperature from 600 °C to 700 °C. At higher temperatures above 700 °C, both the efficiency of the produced biochar reduce and a gasification process takes place rather than a pyrolysis process. Therefore, it has not been studied at higher temperature and the highest BET surface area value for biochar obtained from the walnut shell was reached at 700 ° C. In order to use the produced biochar as an adsorbent, it is necessary to have a high surface area. In this context, the removal of Cu(II) ions from aqueous solutions was investigated using hazelnut shell carbonized at 500 °C and walnut shell carbonized at 700 °C.

Determination of adsorption capacity of biochars

Effect of initial solution pH and temperature

As is known, heavy metals are usually dissolved in water at neutral and acidic pH values. At basic pH values, the metal ions in the water react with the hydroxide ions in the environment and precipitate as metal hydroxides (Barakat 2011). The original pH of the copper solution used in this study was 2.5. For experiments to be carried out at different pH, initially the pH of the starting copper solution was adjusted from acidic medium to basic conditions. However, while performing this process, it was observed that the dissolved copper ions in the environment started to precipitate as copper hydroxide after pH 5. Due to the occurrence of the chemical precipitation process, pH values higher than pH 5 could not be studied. Additionally, it is a known fact that at low pH values (pH < 2.5), protonation of the functional groups on the biochar surface occurs, and thereby the adsorbent surface becomes positively charged. Due to the absence of electrostatic interaction between the positively charged surface of the adsorbent and the Cu(II) ions, adsorption efficiency will be very low under pH 2.5. Therefore, the adsorption process was carried out in an acidic medium, changing pH between 2.5 and 5 and in the experimental conditions of $C_0 =$ 15 ppm, adsorbent amount = 3 g/L, T = 25 °C and mixing speed = 600 rpm. Heavy metal removal efficiency (%) achieved for both biochar produced from hazelnut shell (HSC) and walnut shell (WSC) is given in Figure 4(a). Experimental results showed that the concentration of Cu(II) ions

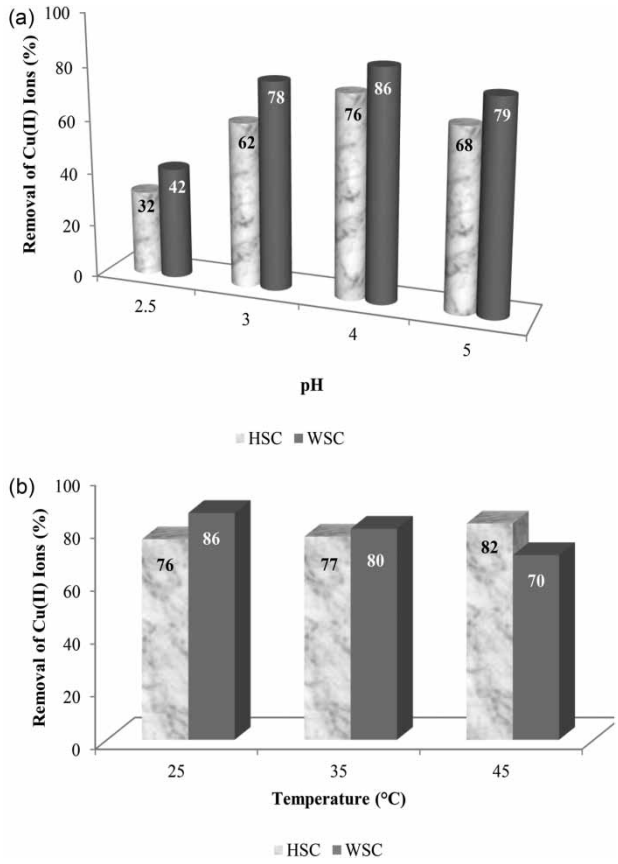

Figure 4 | (a) The adsorption efficiencies (%) achieved in the removal of Cu(II) ions from aqueous solutions at different pH values; (b) adsorption efficiency reached in the removal of Cu(II) ions from aqueous solutions at different temperatures ($C_0 = 15$ ppm; adsorbent dosage = 3 g/L; pH = 4; mixing speed = 600 rpm).

in the solution at equilibrium differ significantly from each other according to the pH value of the solution. Adsorption was strongly influenced by solution pH due to the hydronium or hydroxyl ions, which adsorbed strongly compared to other ions in the medium. The hydronium ions predominant in the medium at low pH values were more interested in the active centers on the surface of the adsorbent than the Cu(II) ions, which have a positive charge in solution. For this reason, the surface of the adsorbent was positively charged, which reduced the electrostatic attraction between the adsorbent surface and heavy metal ions. However, the decrease in concentration of hydronium ions in the medium with increasing pH or the increase in the concentration of negatively charged hydroxyl ions also resulted in an increase in the adsorption capacity for positively charged Cu(II) ions. Because at high pH values the attraction between the negatively charged adsorbent surface and the positively charged Cu(II) ions was increased (Dowlatshahi *et al.* 2014; Imamoglu *et al.* 2018). However, the increase in both the yield and the adsorption capacity continued until pH 4, after which Cu(II) ions tended to precipitate as hydroxides at higher pH values, especially after pH 5. As a result, the highest removal efficiency and adsorption capacity for Cu(II) ions was reached at pH 4 and adsorption efficiency decreased when alkali values were approached (Safinejad *et al.* 2017). Consequently, the adsorption process was performed due to electrostatic attractions between the biochar's surface and Cu(II) ions. Since the adsorbents provided high treatment efficiency at pH 4, all the further studies were carried out at this pH.

Experimental results have shown that the surface charge of the adsorbent and hence the adsorption capacity varies greatly depending on the pH of the solution. Similar conclusions have been reached in the literature. The pH value of the solution has an important role in the adsorption process not only for electrostatic interaction and/or the surface charge of an adsorbent but also hydrogen bond formation, electron exchange and π-π dispersion interactions in solution (Lemraski & Sharafinia 2016).

In the adsorption process, temperature is a very important parameter in terms of not only efficiency but also characterization of the adsorption type. The adsorption efficiencies (%) of Cu(II) ions in aqueous solutions at three different temperatures using biochar obtained from hazelnut and walnut shell are shown in Figure 4(b). Experimental results showed that the adsorption efficiency for Cu(II) ions increased with the increase of temperature in studies using biochar obtained from hazelnut shell. This increase in the aqueous solution temperature reduced the activation energy barrier that must be exceeded for the adsorption process to occur and increased the interactions between the metal ions and the adsorbent surface (Jonasi *et al.* 2017). Therefore, this increase in the efficiency of adsorption with increasing temperature indicated that the process was endothermic. However, in studies using biochar obtained from walnut shell, a significant decrease in the adsorption efficiency of Cu(II) ions was observed with increasing temperature. Generally, the increase in the adsorption capacity with increasing temperature shows that the process is chemical, and vice versa, the adsorption process is physical. Therefore, the decrease in adsorption efficiency with increasing

temperature indicated that the process was exothermic and that a reversible physical adsorption process, which is the resultant weak bond between the molecules, took place.

Effect of initial copper concentration and adsorbent dosage

In the adsorption process, which expresses adherence to surface, the most important driving force between the liquid and solid phase is undoubtedly the initial concentration. When the biochar obtained from the hazelnut shell is used as an adsorbent, the effect of different initial Cu(II) concentrations on adsorption yield and adsorption capacity values are shown in Figure 5(a) as an example. Experimental results showed that by changing the initial concentration of Cu(II) ions in the range of 15–45 ppm, the adsorption efficiency decreased, whereas the adsorption capacity values increased. Similar results were obtained in

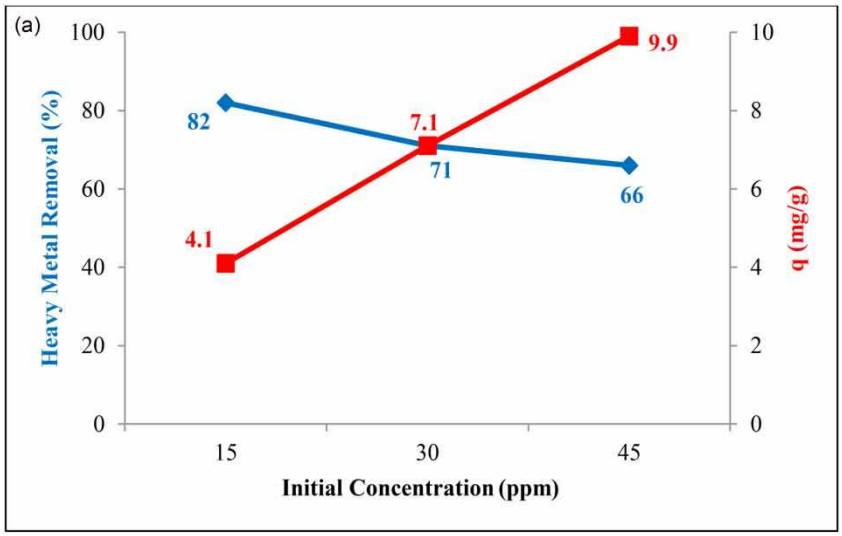

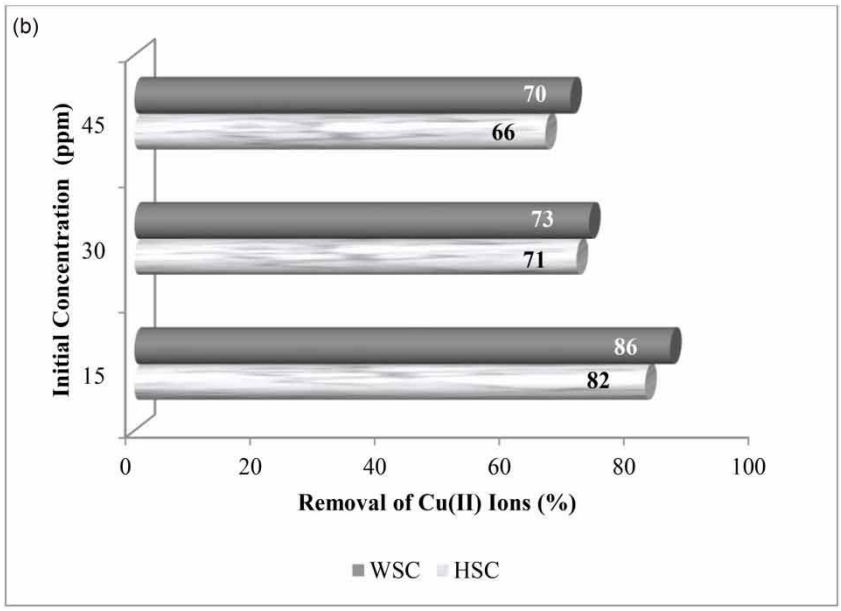

Figure 5 | (a) The adsorption efficiency and adsorption capacity values for different initial heavy metal concentrations (adsorbent type = HSC; pH = 4; adsorbent dosage = 3 g/L; T = 45 °C; mixing speed = 600 rpm); (b) the adsorption yields achieved at different initial concentrations of Cu(II) ions (pH = 4; adsorbent dosage = 3 g/L; mixing speed = 600 rpm; T = 45 °C for HSC; T = 25 °C for WSC).

studies using biochar obtained from walnut shell. Experimental results were consistent with similar studies in the literature, and all molecules in the solution, particularly at low concentrations, interacted with the binding sites of the adsorbent, resulting in high removal efficiencies due to the limited number of binding sites of all adsorbents saturated at a given concentration. However, since the initial concentration is an important driving force for the mass transfer between the aqueous solution and the solid phase to overcome the resistance, the increased initial concentration caused an increase in the equilibrium adsorption capacity (Chowdhury *et al.* 2011). Figure 5(b) shows the maximum removal efficiencies obtained for both adsorbents at different initial heavy metal concentrations. From the experimental results, it was obvious that the adsorption efficiency decreased with increasing initial concentration for Cu(II) ions.

The increase in the amount of adsorbent sometimes causes a decrease in the adsorption value and sometimes it has a positive effect of increasing the adsorption. If the active sites of the adsorbent surface during adsorption remain unfilled by the ions to be removed from the aqueous solution, a decrease in adsorption value may be seen (Bulut & Aydın 2005; Bulut *et al.* 2006). By using the biochar obtained from hazelnut and walnut shell as adsorbent, the adsorption yields of Cu(II) ions removed from the aqueous solution in different adsorbent amounts are shown in Figure 6. It was obvious that the adsorption efficiency for Cu(II) ions increased with increasing adsorbent amount from experimental results. The highest percentage of removal of Cu(II) metal ions was obtained at 3 g/L. It was believed that the adsorption efficiency was increased due to the increase in the surface area of the adsorbent in contact with the ions in the solution. This was because increasing the adsorbent dose allows a large surface area to be formed for adsorption (Changmai *et al.* 2018). For this reason, the determination of different adsorption yield values for both adsorbents suggested that the adsorbents may result from differences in surface areas. In addition, the presence of more active binding sites in the medium with increasing adsorbent dosage was another factor that positively affected the adsorption process.

Effect of mixing speed and contact time

In order to reach the maximum adsorption capacity in the adsorption process, it is very important to ensure that the adsorbent is dispersed in the solution in an effective and homogeneous manner, even if the fixed film layer on the adsorbent surface is thin. At this point, the speed of mixing is confronted as one of the parameters affecting the adsorption process. The results obtained from the adsorption experiments carried out by changing the mixing speed between 200 and 600 rpm are given in Figure 7. Experimental results showed that the adsorption yield values of Cu(II) metal ions increased with increasing mixing speed. This

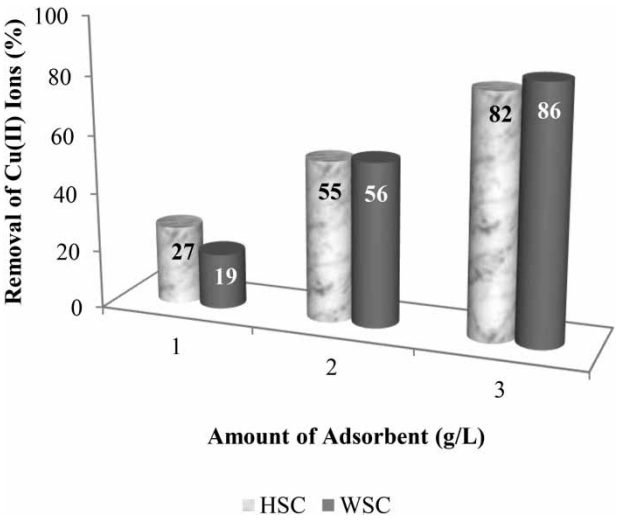

Figure 6 | The adsorption efficiencies achieved in the removal of Cu(II) ions from aqueous solutions at different adsorbent amounts ($C_0 = 15$ ppm; pH = 4; mixing speed = 600 rpm; T = 45 °C for HSC; T = 25 °C for WSC).

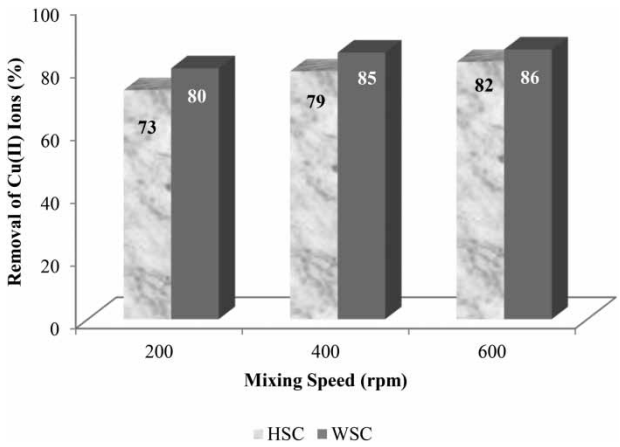

Figure 7 | Adsorption yields obtained from removal of Cu(II) ions from aqueous solutions at different mixing speed ($C_0 = 15$ ppm; pH = 4; adsorbent dosage = 3 g/L; T = 45 °C for HSC; T = 25 °C for WSC).

result could be explained by the fact that as the mixing speed increased, the fixed film layer around the adsorbent was thinned by deformation and the thinner this layer was, the easier it would be for the copper ions to pass through this layer and stick to the adsorbent surface. However, as the mixing speed increased, the interaction between the copper ions and the functional groups on the adsorbent surface would increase as the possibility of molecular collision in the solution increased (Masiya & Gudyanga 2009). As a result, the increase in the mixing speed increased the adsorption efficiency because it had a positive effect of interaction between the active sites of the adsorbent surface and the copper ions. However, the experimental results obtained from very high mixing speeds (at 600 rpm) did not cause a sharp increase in adsorption, especially when compared to the results of adsorption studies that were carried out usually between 150 and 200 rpm in the literature. It has been found that the adsorption efficiency of Cu(II) metal ions increases significantly with increasing mixing speed, especially from 200 to 400 rpm.

Adsorption is a process that continues until a dynamic equilibrium is established between the dissolved concentration remaining in the solution and the dissolved concentration retained on the solid surface. Therefore, the optimum contact time or duration of the equilibrium for adsorption can be determined by determining the heavy metal concentration remaining in the solution in samples taken at specific time intervals. Table 2 gives the amounts of solute adsorbed per unit mass of the adsorbent at the time of equilibrium and optimum contact time in the removal of Cu(II) ions from aqueous solutions at optimum conditions and different heavy metal concentrations. Experimental results indicated that the duration of the equilibrium increased with increasing initial heavy metal concentration. However, if the adsorption rates of Cu(II) ions onto two different adsorbents are compared, Cu(II) ions were adsorbed faster when using HSC as adsorbent, and adsorption was completed within 30 min and a faster equilibrium state was reached. Particularly rapid adsorption and short time to reach equilibrium is an important parameter showing the effectiveness of this adsorbent to be used in water treatment. When using WSC as adsorbent, the time of equilibrium in the aqueous solution containing Cu(II) ion was determined to be 75 min for each of the three concentrations studied. When the equilibrium was reached, there was no change in the adsorption capacities.

Table 2 | The values of q_e (mg/g) reached at equilibrium and optimum contact time for removal of Cu(II) ions from aqueous solution (pH = 4, adsorbent dosage = 3 g/L; mixing speed = 600 rpm; T = 45 °C for HSC; T = 25 °C for WSC)

		Cu(II)	
Adsorbent type	**C (ppm)**	**q_e (mg/g)**	**Duration of equilibrium (min)**
HSC	15	4.1	8
	30	7.1	20
	45	9.9	30
WSC	15	4.3	75
	30	7.2	75
	45	11.1	75

Although the adsorption capacities of the biochars (q_e) were lower than some adsorbents in the literature, it should be remembered that the capacity of these cheap and environmentally friendly materials can be increased by chemical activation. Chemical activation can be carried out using suitable acid, base and metal salts. The main purpose of acid activation is to remove the unwanted metals from the biochar's structure and bond the functional groups in the acid to the biochar surface. Hydrochloric acid, sulfuric acid, nitric acid, phosphoric acid, oxalic acid and citric acid are among the most used acids in the literature for acid activation. The main purpose of activation with the base is to increase the surface area of the biochar and the functional groups it contains, as in acid activation. Common compounds used for base activation are potassium hydroxide and sodium hydroxide.

Adsorption isotherm models

Adsorption isotherms show how adsorbed molecules distribute between the solid and liquid phases when equilibrium is reached in the adsorption process. Therefore, with the help of experimental data obtained from adsorption studies, it is very important to determine the best isotherm model that the results are compatible with in order to explain the nature and processes of the adsorption process (Thajeel 2013). The equilibrium concentration (C_e) and equilibrium adsorption capacity (q_e) values for Cu(II) ions are given in Table 3 as a result of adsorption performed at different

Table 3 | The values of C_e (ppm) and q_e (mg/g) at different temperature and different initial heavy metal concentration values

			T = 25 °C		T = 35 °C		T = 45 °C	
Adsorbent type	**Heavy metal**	**C_o (ppm)**	**C_e**	**q_e**	**C_e**	**q_e**	**C_e**	**q_e**
HSC	Cu(II)	15	3.55	3.80	3.41	3.85	2.80	4.07
		30	10.93	6.63	10.50	6.72	8.60	7.10
		45	19.26	9.25	18.50	9.37	15.20	9.90
WSC	Cu(II)	15	2.10	4.30	3.00	4.00	4.50	3.50
		30	3.78	8.85	5.40	8.23	8.10	7.20
		45	5.27	13.76	7.53	12.80	11.30	11.20

temperatures and different initial heavy metal concentrations using biochar obtained from hazelnut and walnut shells. The compatibility of these experimental data with the Langmuir, Freundlich and Temkin isotherm models was investigated.

The linear form of the Langmuir (Equation (3)), Freundlich (Equation (4)) and Temkin (Equation (5)) equations are commonly given by:

$$\frac{C_e}{q_e} = \frac{C_e}{q_{max}} + \left(\frac{1}{q_{max} K_L}\right) \tag{3}$$

$$\ln q_e = \ln K_f + \frac{1}{n} \ln C_e \tag{4}$$

$$q_e = B \ln A + B \ln C_e \tag{5}$$

where C_e is the equilibrium concentration of solute in the bulk solution (mg/L), q_e is the amount of solute adsorbed per unit mass of adsorbent (mg/g), q_m is the maximum adsorption capacity (mg/g), K_L is the constant related to the free energy of adsorption (L/mg), K_f is a Freundlich constant indicative of the relative adsorption capacity of the adsorbent [mg/g $(L/mg)^{1/n}$], 1/n is the heterogeneity factor, which is the constant characteristics of the system, A is the Temkin isotherm equilibrium binding constant (L/g) and B is the constant related to heat of sorption (J/mol) (Dada *et al.* 2012).

With the application of the results obtained experimentally to the Langmuir, Freundlich and Temkin isotherm models, the linear isotherm graphs C_e/q_e versus C_e, $\ln q_e$ versus $\ln C_e$, q_e versus $\ln C_e$ were drawn and the model parameters calculated from these graphs are given in Tables 4–6.

Table 4 | The Langmuir isotherm constants for Cu(II) adsorption

Adsorbent type	**Heavy metal**	**T (°C)**	**R^2**	**q_{max} (mg/g)**	**K_L (L/mg)**	**$q_{exp.}$ (mg/g)**
HSC	Cu(II)	25	0.969	13.77	0.098	3.80
		35	0.969	13.95	0.102	3.85
		45	0.970	14.73	0.125	4.07
WSC	Cu(II)	25	0.996	30.03	0.060	4.30
		35	0.997	27.93	0.042	4.00
		45	0.996	24.51	0.028	3.50

Table 5 | The Freundlich isotherm constants for Cu(II) adsorption

Adsorbent type	**Heavy metal**	**T (°C)**	**R^2**	**K_f [mg/g $(L/mg)^{1/n}$]**	**n (g/L)**	**1/n**
HSC	Cu(II)	25	0.998	1.947	1.916	0.522
		35	0.998	2.015	1.917	0.522
		45	0.998	2.362	1.918	0.521
WSC	Cu(II)	25	0.999	1.003	0.794	1.259
		35	0.999	1.680	0.794	1.259
		45	0.999	1.908	0.794	1.259

Table 6 | Temkin model parameters for Cu(II) adsorption

Adsorbent type	**Heavy metal**	**T (°C)**	**R^2**	**A**	**B**
HSC	Cu(II)	25	0.973	1.111	3.123
		35	0.973	1.066	3.164
		45	0.974	1.143	3.342
WSC	Cu(II)	25	0.968	1.414	9.989
		35	0.968	2.020	9.290
		45	0.968	3.030	8.125

It is clear from Table 4 that maximum adsorption capacity (q_{max}) values calculated for Cu(II) ions at different temperatures by isotherm graphs increase with temperature

when HSC was used as an adsorbent and decrease with temperature when WSC was used as an adsorbent. The fact that the q_{max} (mg/g) values calculated by Langmuir isotherms are higher than the experimentally determined q_{exp} (mg/g) values for Cu(II) ions at different temperatures suggests that the carbon-based adsorbent surface is not completely covered by copper ions. The high correlation coefficients (R^2) values, however, indicate that the adsorption process may be compatible with the Langmuir isotherm model, indicating that Cu(II) ions may be monolayer bonded on a carbon-based adsorbent.

As is seen from Table 5, if the biochar obtained from the hazelnut shell is used as an adsorbent, the adsorption process is a chemical process because of the fact that 1/n values are smaller than 1. When the biochar obtained from the walnut shell is used as an adsorbent, it can be said that a physical adsorption process is performed because the 1/n values are larger than 1. These results are similar to those obtained by studies on the effect of temperature on the adsorption process in order to characterize the adsorption model. The value of the K_f constant showing the adsorption capacity increases with increasing temperature for both biochars used as adsorbents in the removal of Cu(II) ions. Therefore, the increase in the K_f value with temperature indicates that the adsorption rate increases with increasing temperature. When the R^2 values, which are the most important parameter in determining the suitability of the experimental data to the isotherm model, are examined, it is seen from Table 5 that this value is very close to 1. When the correlation coefficients are taken into consideration, it is seen that the Freundlich model gives better results than the Langmuir model.

When the correlation coefficients are examined in determining the suitability of the experimental data for the Temkin isotherm model (Table 6), high R^2 values were obtained in Cu(II) ions for both adsorbents. For this reason, it can be concluded that the experimental results may be compatible with the Temkin isotherm model.

However, when all the isotherm models of Langmuir, Freundlich and Temkin are evaluated together, the experimental results obtained from the use of biochar as produced from hazelnut and walnut shells as adsorbents are more similar to the Freundlich isotherm model with the correlation coefficients ($R^2 \geq 0.99$) being close to 1 has been achieved. The Freundlich isotherm is based on the assumption that the adsorbent has a heterogeneous surface composed from different classes of adsorption sites. So, it indicates multilayer sorption of the surface. This adsorption isotherm provide some insight into the adsorption mechanism and the surface characteristics of adsorbents.

Adsorption kinetics modeling

In order to examine the mechanism of the adsorption process, pseudo first order, pseudo second order and intra-particle diffusion adsorption models were used to adjust kinetic experimental data. The linear form of pseudo first order, pseudo second order and intra-particle diffusion rate equations are presented in Equations (6)–(8), respectively.

$$\log(q_e - q_t) = \log(q_e) - \frac{k_1}{2,\ 303}t \tag{6}$$

$$\frac{t}{q_t} = \frac{1}{k_2 q_e^2} + \frac{t}{q_e} \tag{7}$$

$$q_t = k_i.t^{1/2} + C \tag{8}$$

where q_t and q_e denote the sorption capacity (mg/g) at a given time and at equilibrium, respectively, k_1 is the pseudo first order rate constant (min^{-1}), k_2 is the pseudo second order rate constant ($g\,mg^{-1}\,min^{-1}$), k_i is the intra-particle diffusion rate constant ($mg/g.dk^{0.5}$), C is the constant and t is the time (min) (Doğan *et al.* 2009).

The linear graphs of $\log(q_e - q_t)$ versus t, t/q_t versus t and q_t versus $t^{0.5}$ were drawn (Figure 8) and the values of kinetic parameters (the rate constants of the three models with the correlation coefficients and theoretical adsorption capacity values) of the linear form of rate equations are presented in Tables 7–9.

As can be seen from Table 7, as the temperature increases in the adsorption of Cu(II) ions on the biochar obtained from hazelnut shell, the q_e values obtained from the model equations and also the $q_{exp.}$ values calculated by the experimental data are increased while the rate constant (k_1) is decreasing. This result shows that as the temperature increases, greatly adsorption occurs but it is more slowly than lower temperatures. As the temperature increases in the adsorption of Cu(II) ions on the biochar obtained from

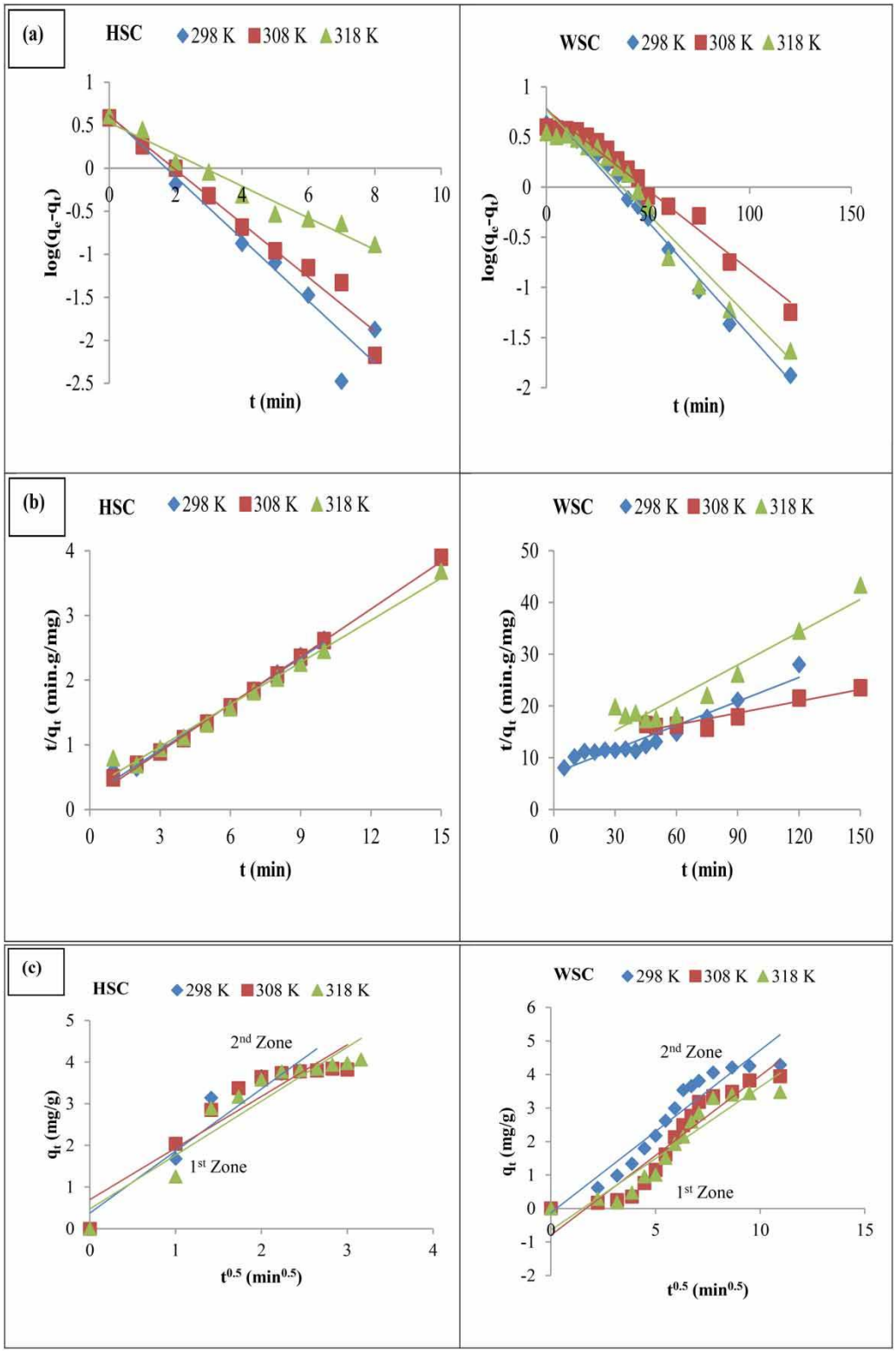

Figure 8 | Kinetic model curves obtained at different temperature values (a) pseudo first order kinetic model, (b) pseudo second order kinetic model, (c) intra-particle diffusion kinetic model.

Table 7 | Constants for the pseudo first order kinetic model

Adsorbent type	Heavy metal	T (°C)	k_1 (min^{-1})	q_e (mg/g)	R^2	$q_{exp.}$ (mg/g)
HSC	Cu(II)	25	0.829	3.39	0.936	3.80
		35	0.720	4.05	0.974	3.85
		45	0.425	4.15	0.966	4.07
WSC	Cu(II)	25	0.037	6.12	0.986	4.30
		35	0.048	5.90	0.974	4.00
		45	0.052	5.89	0.955	3.50

Table 8 | Constants for the pseudo second order kinetic model

Adsorbent type	Heavy metal	T (°C)	R^2	k_2 (g/mg.min)	q_e (mg/g)	$q_{exp.}$ (mg/g)
HSC	Cu(II)	25	0.992	0.353	4.08	3.80
		35	0.998	0.286	4.22	3.85
		45	0.987	0.147	4.61	4.07
WSC	Cu(II)	25	0.927	0.001	9.165	4.30
		35	0.896	0.002	7.483	4.00
		45	0.912	0.005	5.916	3.50

Table 9 | Constants for the intra-particle diffusion kinetic model

Adsorbent type	Heavy metal	T (°C)	R^2	k_i ($mg/g.min^{0.5}$)	C
HSC	Cu(II)	25	0.909	1.191	0.376
		35	0.872	1.239	0.698
		45	0.888	1.296	0.473
WSC	Cu(II)	25	0.913	0.485	0.129
		35	0.898	0.476	0.797
		45	0.891	0.428	0.647

walnut shell, the rate constant (k_1) increases while the q_e values obtained from the model equations or the $q_{exp.}$ values calculated by the experimental data are decreased. This result shows that as the temperature increases, the amount of copper ions adsorbed decreases, but the adsorption rate increases according to lower temperatures; that is, the adsorption takes place faster. However, the q_{exp} values obtained experimentally and the q_e values obtained from the model equations are close to each other and the correlation coefficient values are close to 1, indicating that the pseudo first order kinetic model may be suitable for this system.

As can be seen from Table 8, as the temperature increases in the adsorption of Cu(II) ions on the biochar obtained from hazelnut shell, the q_e values obtained from the model equations and also the $q_{exp.}$ values calculated by the experimental data are increased while the rate constant (k_2) is decreasing. This result shows that as the temperature increases, the amount of copper ions adsorbed increases but the adsorption process is slower than at lower temperatures. Therefore, the adsorption process is slower at higher temperatures. As the temperature increases in the adsorption of Cu(II) ions on the biochar obtained from walnut shell, the rate constant (k_2) increases while the q_e values obtained from the model equations or the $q_{exp.}$ values calculated by the experimental data are decreased. This result shows that as the temperature increases, the efficiency of the recovery due to the amount of copper ions adsorbed decreases, but the adsorption process takes place faster at higher temperatures. It can be said that this model may be suitable for the working system if the correlation coefficient values obtained by pseudo second order kinetic modeling equation and the difference between $q_{exp.}$ values obtained from experimental data and q_e values obtained from model equations are taken into consideration.

As can be seen from Table 9, as the temperature increases in the adsorption of Cu(II) ions on the biochar obtained from the hazelnut shell, rate constant (k_i) is increased and therefore adsorption is faster at higher temperatures. On the contrary, the decrease in the rate constant with increasing temperature indicates that the adsorption process is slow at high temperatures when using the biochar obtained from walnut shell. However, the application of experimental data to the intra particle diffusion model has resulted in the fact that this model is not suitable for the system because the resultant correlation coefficients are lower when compared to the other two kinetic models.

As a result, it is necessary to evaluate all the results of the pseudo first order kinetic model, the pseudo second order kinetic model and the intra particle diffusion model, and especially the correlation coefficients, in order to accurately determine the kinetic model of the system. The model in which correlation coefficients values are closest to 1 is the most suitable kinetic model for the system and also $q_{exp.}$ (mg/g) values obtained experimentally and q_e (mg/g) values obtained from the model equations are very close to each other. When the results are evaluated in this context and using the HSC as an adsorbent, it is determined that Cu(II) ions adsorption is more appropriate to the pseudo second order kinetic model. In studies where WSC is used as adsorbent, it has been determined that the adsorption of Cu(II) ions is suitable for the pseudo first-order kinetic model. The results are consistent with the literature (Kim *et al.* 2001; Sencan *et al.* 2015; Imamoglu *et al.* 2018).

Since pseudo first order and pseudo second order models do not suggest a definite mechanism for adsorption, the results were analyzed using the intraparticle diffusion model to predict the rate limiting step. There might be one or more controlling steps for the adsorption process such as external diffusion, pore diffusion, surface diffusion, and adsorption on the pore surface, or a combination of more than one step (Ali & Mohamed 2017). As shown in Figure 8(c), the adsorption process takes place by creating two zones. The 1st zone is surface adsorption, while the 2nd zone represents intra-particulate diffusion. Therefore, in the adsorption process in two stages, the Cu(II) ions coming to the film layer in the first stage pass through the stagnant part there, proceed towards the pores of the adsorbent (boundary layer diffusion) and attach to the biochar surface. In the second stage, the Cu(II) ions move into the micro and macro pore cavities of the adsorbent and proceed to the surface of the adsorption (diffusion in the particle) and attach to the surface of the pore. This result revealed that the adsorption process was not controlled by one step for both biochars. In the case of Cu(II) adsorption, the rapid surface adsorption and intraparticle diffusion stage happened together. In other words, intraparticle diffusion was not the only rate-controlling step and the adsorption occurred through a complex mechanism.

Thermodynamic study

The enthalpy (ΔH°), entropy (ΔS°) and free energy (ΔG°) changes for the adsorption process can be determined by means of the equilibrium constant. These thermodynamic parameters are shown in Equations (9)–(11) and are calculated by using the adsorption equilibrium constant values (K_c) (Table 10) determined for different temperatures.

$$\Delta G = -RT\ln K_c \tag{9}$$

$$\ln K_c = -\frac{\Delta H}{RT} + \frac{\Delta S}{R} \tag{10}$$

$$K_C = \frac{C_{ads}}{C_e} \tag{11}$$

where R (8.314 J/mol K) is the universal gas constant, T (K) is the absolute solution temperature, C_{ads} is the adsorbed metal ion concentration at equilibrium and C_e is the concentration of metal ions remaining in the solution at equilibrium. The values of ΔH° and ΔS° were determined from the slope and intercept of the Van 't Hoff plots of $\ln K_c$ versus 1/T, which are shown in Figure 9. The calculated thermodynamics parameters are given in Table 11.

When the thermodynamic parameter values given in Table 11 are examined, it can be seen that Gibbs free energy values for Cu(II) ions are negative in studies using HSC as an adsorbent and that ΔG^o has larger negative values with increasing temperature. A negative Gibbs free energy value indicates that the adsorption process occurs spontaneously. Other thermodynamic parameters, ΔH° and ΔS°, are positive. Entropy and enthalpy values are the values that show the formation of the solid/solution interface during the adsorption process and

Table 10 | Thermodynamic equilibrium constants calculated at different temperatures for Cu(II) ions

Adsorbent type	Heavy metal	T (K)	K_c
HSC	Cu(II)	298	3.225
		308	3.399
		318	4.357
WSC	Cu(II)	298	6.143
		308	4.000
		318	2.333

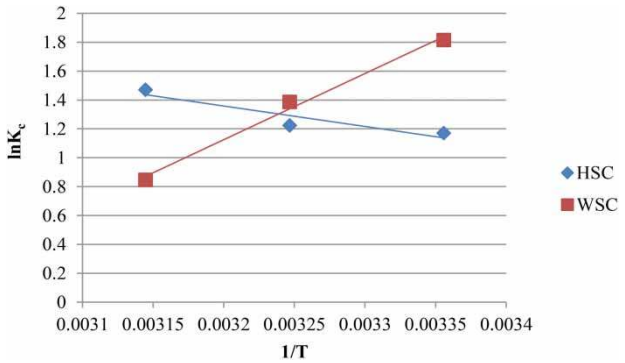

Figure 9 | Adsorption heat diagram for Cu(II) adsorption.

characterize it. Positive ΔH° values indicate the endothermic behavior of the adsorption process (Jonasi *et al.* 2017). The positive ΔS° values obtained for Cu(II) ions in the study have shown that the hold of ions at the solid/solution interface randomly during the adsorption process may be high. In particular, the high positive entropy value of Cu(II) ions reveals that these are better retained at the interface and show more interest in the adsorbent used (Ghasemi *et al.* 2015; Yuşan 2017). When WSC is used as an adsorbent, it is seen that the Gibbs free energy values for Cu(II) ions are again negative and that ΔG^{o} has smaller negative values with increasing temperature. This result shows that the adsorption process occurs spontaneously at all temperatures studied, but the drop in the values of negativity at high temperatures suggests that the spontaneous realization of adsorption may be a little more difficult than at lower temperatures. The ΔH° and ΔS° values are negative for Cu(II) ions. Negative enthalpy values indicate that the adsorption process is exothermic. However, the negative values of ΔS^{o} indicate irregularity during the adsorption process at the solid/solution interface, which is evidence that this irregularity has decreased during the process.

Table 11 | Thermodynamic parameters obtained at different temperature values

Adsorbent type	Heavy metal	T (°C)	ΔH° (kJ/mol)	ΔS° (J/mol·K)	ΔG° (kJ/mol)
HSC	Cu(II)	25	11.76	48.94	−2.901
		35			−3.133
		45			−3.891
WSC	Cu(II)	25	−38.08	−112.50	−4.498
		35			−3.550
		45			−2.240

Surface characteristics of biochars before and after adsorption

In this study, topographic images of the biochar samples used as adsorbent were taken and the morphological change of adsorbent was investigated after the adsorption process. SEM photographs of biochar samples (using HSC as an example) taken before and after adsorption are given in Figure 10. When the SEM photographs taken at different magnification ratios are examined, it is clear that the adsorbents obtained by the pyrolysis process have a very favorable pore structure for the adsorption process and that these pores are empty before adsorption. Surface images taken after adsorption clearly show that the surface of the adsorbent changes considerably after the treatment, and that Cu(II) ions, which are desired to be removed from the aqueous solution in operation, are held by the pores significantly. This is supported by surface images in which the adsorption process has been successfully performed and very high copper removal values have been achieved. Both the experimental results obtained from the batch adsorption process and the morphological changes on the surface after adsorption are in line with each other, and the results are similar to the SEM images in the literature.

CONCLUSIONS

The presence of heavy metals, which have many physiological and toxic effects on living beings, can even put life in danger. For this reason, it is very important to remove heavy metal ions from the aquatic environment by using appropriate treatment techniques. The present paper proposes a green technical approach to the adsorption of copper ions from aqueous solution. With the results of studies made to realize this aim, when the data obtained from the characterization and adsorption studies of biochar obtained from hazelnut and walnut shells are evaluated together, it can be said that the pyrolysis-produced adsorbents of these two biomasses are

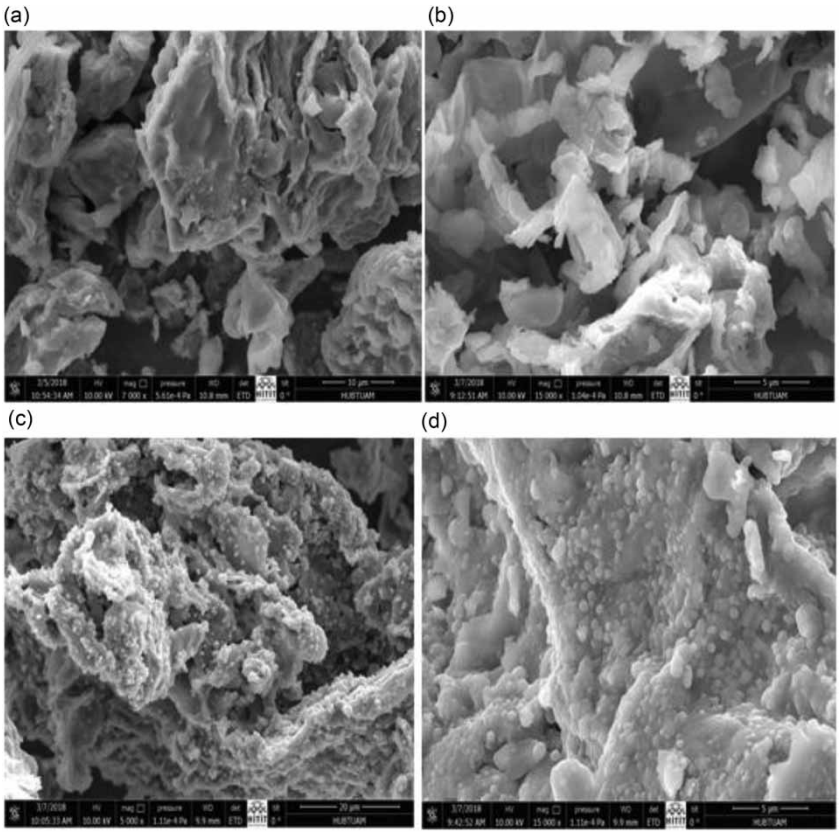

Figure 10 | SEM images of the biochar obtained by using hazelnut shell. SEM images before adsorption (a) x7000, (b) x15000; SEM images after adsorption (c) x5000 (d) x15000.

effective and high-yielding materials for removing copper ions from aqueous solutions. The adsorption process of copper ions is best described by the Freundlich isotherm for both biochars. When using the HSC as an adsorbent, it is determined that copper ions adsorption is more appropriate to the pseudo second order kinetics model. However, in studies where WSC is used as adsorbent, it has been determined that the adsorption process is suitable for the pseudo first-order kinetic model. Experimental results show that both agricultural wastes have been used successfully and support the proposed eco-friendly technical solution for treatment of wastewater. Consequently, the high porosity and high adsorption capacities of the produced biochars show that they will be suitable adsorbents for the removal of heavy metals in water resources. At the same time, they also offer some advantages in terms of agricultural waste assessment and also production of carbon-based adsorbent at lower costs than commercial activated carbon.

ACKNOWLEDGEMENTS

The authors would like to thank Hitit University and Ondokuz Mayıs University for their support.

DATA AVAILABILITY STATEMENT

All relevant data are included in the paper or its Supplementary Information.

REFERENCES

Alalwan, H. A., Kadhom, M. A. & Alminshid, A. H. 2020 Removal of heavy metals from wastewater using agricultural byproducts. *Journal of Water Supply: Research and Technology-Aqua* **69** (2), 99–112.

Ali, O. & Mohamed, S. 2017 Adsorption of copper ions and alizarin red S from aqueous solutions onto a polymeric

nanocomposite in single and binary systems. *Turkish Journal of Chemistry* **41**, 967–986.

Alkherraz, A. M., Ali, A. K. & Elsherif, K. M. 2020 Removal of Pb (II), Zn (II), Cu (II) and Cd (II) from aqueous solutions by adsorption onto olive branches activated carbon: equilibrium and thermodynamic studies. *Chemistry International* **6**, 11–20.

Amarasinghe, B. & Williams, R. 2007 Tea waste as a low cost adsorbent for the removal of Cu and Pb from wastewater. *Chemical Engineering Journal and the Biochemical Engineering Journal* **132**, 299–309.

Balasundram, V., Ibrahim, N., Kasmani, R. M., Hamid, M. K. A., Isha, R., Hasbulla, H. & Rasit Ali, R. 2017 Thermogravimetric catalytic pyrolysis and kinetic studies of coconut copra and rice husk for possible maximum production of pyrolysis oil. *Journal of Cleaner Production* **167**, 218–228.

Barakat, M. A. 2011 New trends in removing heavy metals from industrial wastewater. *Arabian Journal of Chemistry* **4**, 361–377.

Ben-Ali, S., Jaouali, I., Souissi-Najar, S. & Ouederni, A. 2017 Characterization and adsorption capacity of raw pomegranate peel biosorbent for copper removal. *Journal of Cleaner Production* **142**, 3809–3821.

Bulut, Y. & Aydın, H. 2005 A kinetics and thermodynamics study of methylene blue adsorption on wheat shells. *Desalination* **194**, 259–267.

Bulut, Y., Gözübenli, N. & Aydın, H. 2006 Equilibrium and kinetics studies for adsorption of direct blue 71 from aqueous solution by wheat shells. *Journal of Hazardous Materials* **144** (1–2), 300–306.

Changmai, M., Banerjee, P., Nahar, K. & Purkait, M. K. 2018 A novel adsorbent from carrot, tomato and polyethylene terephthalate waste as a potential adsorbent for Co(II) from aqueous solution: kinetic and equilibrium studies. *Journal of Environmental Chemical Engineering* **6**, 246–157.

Chowdhury, S., Chakraborty, S. & Saha, P. 2011 Biosorption of basic green 4 from aqueous solution by Ananas comosus (pineapple) leaf powder. *Colloids and Surfaces B: Biointerfaces* **84**, 520–527.

Dada, A. O., Olalekan, A. P., Olatunya, A. M. & Dada, O. 2012 Langmuir, Freundlich, Temkin and Dubinin–Radushkevich isotherms studies of equilibrium sorption of Zn^{2+} unto phosphoric acid modified rice husk. *IOSR Journal of Applied Chemistry* **3** (1), 38–45.

Dawood, S., Sen, T. K. & Phan, C. 2017 Synthesis and characterization of slow pyrolysis pine cone bio-char in the removal of organic and inorganic pollutants from aqueous solution by adsorption: kinetic, equilibrium, mechanism and thermodynamic. *Bioresource Technology* **246**, 76–81.

Demiral, I. & Aydın Şamdan, C. 2016 Preparation and characterisation of activated carbon from pumpkin seed shell using H_3PO_4. *Anadolu University Journal of Science and Technology A-Applied Sciences and Engineering* **17** (1), 125–138.

Doğan, M., Abak, H. & Alkan, M. 2009 Adsorption of methylene blue onto hazelnut shell: kinetic, mechanism and activation parameters. *Journal of Hazardous Materials* **164**, 172–181.

Dowlatshahi, S., Torbati, A. R. H. & Loloei, M. 2014 Adsorption of copper, lead and cadmium from aqueous solutions by activated carbon prepared from saffron leaves. *Environmental Health Engineering and Management Journal* **1** (1), 37–44.

Fazal-ur-Rehman, M. 2018 Methodological trends in preparation of activated carbon from local sources and their impacts on production: a review. *Chemistry International* **4**, 109–119.

Gaouar-Yadi, M., Tizaoui, K., Gaouar-Benyelles, N. & Benguella, B. 2016 Efficient and eco-friendly adsorption using low-cost natural sorbents in waste water treatment. *Indian Journal of Chemical Technology* **23**, 204–209.

Ghaffar, S. H. & Fan, M. 2013 Structural analysis for lignin characteristics in biomass straw. *Biomass and Bioenergy* **57**, 264–279.

Ghasemi, M., Ghoreyshi, A. A., Younesi, H. & Khoshhal, S. 2015 Synthesis of a high characteristics activated carbon from walnut shell for the removal of Cr(VI) and Fe(II) from aqueous solution: single and binary solutes adsorption. *Iranian Journal of Chemical Engineering* **12** (4), 28–51.

Ghrab, S., Benzina, M. & Lambert, S. D. 2017 Copper adsorption from wastewater using bone charcoal. *Advances in Materials Physics and Chemistry* **7**, 139–147.

Gonçalves, G. C., Pereira, N. C. & Veit, M. T. 2016 Production of bio-oil and activated carbon from sugarcane bagasse and molasses. *Biomass and Bioenergy* **85**, 178–185.

Hossain, M., Ngo, H., Guo, W. & Setiadi, T. 2012 Adsorption and desorption of copper (II) ions onto garden grass. *Bioresource Technology* **121**, 386–395.

Imamoglu, M., Öztürk, A., Aydın, Ş., Manzak, A., Gündoğdu, A. & Duran, C. 2018 Adsorption of Cu(II) ions from aqueous solution by hazelnut husk activated carbon prepared with potassium acetate. *Journal of Dispersion Science and Technology* **39** (8), 1144–1148.

Ince, M., Ince, O., Asam, E. & Onal, A. 2017 Using food waste biomass as effective adsorbents in water and wastewater treatment for Cu (II) removal. *Atomic Spectroscopy* **38**, 142–148.

Iqbal, M., Saeed, A. & Kalim, I. 2009 Characterization of adsorptive capacity and investigation of mechanism of Cu^{2+}, Ni^{2+} and Zn^{2+} adsorption on mango peel waste from constituted metal solution and genuine electroplating effluent. *Separation Science and Technology* **44**, 3770–3791.

Jian, X., Zhuang, X., Li, B., Xu, X., Wei, Z., Song, Y. & Jiang, E. 2018 Comparison of characterization and adsorption of biochars produced from hydrothermal carbonization and pyrolysis. *Environmental Technology & Innovation* **10**, 27–35.

Jonasi, V., Matina, K. & Guyo, U. 2017 Removal of Pb(II) and Cd(II) from aqueous solution using alkaline-modified pumice stone powder (PSP): equilibrium, kinetic, and

thermodynamic studies. *Turkish Journal of Chemistry* **41**, 748–759.

Karabelli, D., Ünal, S., Shahwan, T. & Eroğlu, A. E. 2011 Preparation and characterization of alumina-supported iron nanoparticles and its application for the removal of aqueous Cu^{2+} ions. *Chemical Engineering Journal* **168**, 979–984.

Kim, J. W., Sohn, M. H., Kim, D. S., Sohn, S. M. & Kwon, Y. S. 2001 Production of granular activated carbon from waste walnut shell and its adsorption characteristics for Cu^{2+} ion. *Journal of Hazardous Materials* **85**, 301–315.

Legrouri, K., Khouya, E., Hannache, H., El Hartti, M., Ezzine, M. & Naslain, R. 2017 Activated carbon from molasses efficiency for Cr (VI), Pb (II) and Cu (II) adsorption: a mechanistic study. *Chemistry International* **3**, 301–310.

Lemraski, E. H. & Sharafinia, S. 2016 Kinetics, equilibrium and thermodynamics studies of Pb^{2+} adsorption onto new activated carbon prepared from Persian mesquite grain. *Journal of Molecular Liquids* **219**, 482–492.

Liu, S., Chen, X., Liu, A., Wang, L. & Yu, G. 2015 Co-pyrolysis characteristic of biomass and bituminous coal. *Bioresource Technology* **179**, 414–420.

Masiya, T. T. & Gudyanga, F. P. 2009 Investigation of granular activated carbon from peach stones for gold adsorption in acidic thiourea. In: *Proceedings of Hydrometallurgy Conference*, Johannesburg, South Africa, pp. 465–474.

Muhammad, S. A., Muhammad, A. M., Ayed, O. S., Ye, G. B., Luo, H., Ibrahim, M., Rashid, U., Arbi, I. & Qadir, N. G. 2017 Kinetic analyses and pyrolytic behavior of Para grass (Urochloa mutica) for its bioenergy potential. *Bioresource Technology* **224**, 708–713.

Niu, Z., Liu, G., Yin, H., Wu, D. & Zhou, C. 2016 Investigation of mechanism and kinetics of non-isothermal low temperature pyrolysis of perhydrous bituminous coal by in-situ FTIR. *Fuel* **172**, 1–10.

Odeh, A. O. 2015 Qualitative and quantitative ATR-FTIR analysis and its application to coal char of different ranks. *Journal of Fuel Chemistry and Technology* **43**, 129–137.

Park, J. H., Wang, J. J., Kim, S. H., Cho, J. S., Kang, S. W., Delaune, R. D., Han, K. J. & Seo, D. C. 2017 Recycling of rice straw through pyrolysis and its adsorption behaviors for Cu and Zn ions in aqueous solution. *Colloids and Surfaces A* **533**, 330–337.

Plis, A., Lasek, J., Skawinska, A. & Zuwała, J. 2015 Thermochemical and kinetic analysis of the pyrolysis process in *Cladophora glomerata* algae. *Journal of Analytical and Applied Pyrolysis* **115**, 166–174.

Safinejad, A., Chamjangali, M. A., Goudarzi, N. & Bagherian, G. 2017 Synthesis and characterization of a new magnetic bio-adsorbent using walnut shell powder and its application in ultrasonic assisted removal of lead. *Journal of Environmental Chemical Engineering* **5**, 1429–1437.

Saidur, R., Abdelaziz, E. A., Demirbas, A., Hossain, M. S. & Mekhilef, S. 2011 A review on biomass as a fuel for boilers. *Renewable and Sustainable Energy Reviews* **15**, 2262–2289.

Şencan, A., Karaboyacı, M. & Kılıç, M. 2015 Determination of lead(II) sorption capacity of hazelnut shell and activated carbon obtained from hazelnut shell activated with $ZnCl_2$. *Environmental Science and Pollution Sensing, Monitoring, Modeling and Remediation* **22**, 3238–3248.

Sha, L., Xueyi, G., Ningchuan, F. & Qinghua, T. 2009 Adsorption of Cu^{2+} and Cd^{2+} from aqueous solution by mercapto-acetic acid modified orange peel. *Colloids Surf. B Interfaces* **73**, 10–14.

Shen, B., Tian, L., Li, F., Zhang, X., Xu, H. & Singh, S. 2016 Elemental mercury removal by the modified bio-char from waste tea. *Fuel* **187**, 189–196.

Soyler, N., Goldfarb, J. L., Ceylan, S. & Saçan, M. T. 2017 Renewable fuels from pyrolysis of *Dunaliella tertiolecta*: an alternative approach to biochemical conversions of microalgae. *Energy* **120**, 907–914.

Tchounwou, P. B., Yedjou, C. G., Patlolla, A. K. & Sutton, D. J. 2012 Heavy metal toxicity and the environment. In: *Molecular, Clinical and Environmental Toxicology. Experientia Supplementum*, Vol. 101 (A. Luch, ed.). Springer, Basel.

Thajeel, A. S. 2013 Isotherm, kinetic and thermodynamic of adsorption of heavy metal ions onto local activated carbon. *Aquatic Science and Technology* **1** (2), 53–77.

Uzun, B. B. & Yaman, E. 2017 Pyrolysis kinetics of walnut shell and waste polyolefins using thermogravimetric analysis. *Journal of the Energy Institute* **90**, 825–837.

Vukelic, D., Boskovic, N., Agarski, B., Radonic, J., Budak, I., Pap, S. & Sekulic, M. T. 2018 Eco-design of a low-cost adsorbent produced from waste cherry kernels. *Journal of Cleaner Production* **174**, 1620–1628.

Wang, X. S., Li, Z. Z. & Sun, C. 2009 A comparative study of removal of Cu (II) from aqueous solutions by locally low-cost materials: marine macroalgae and agricultural by-products. *Desalination* **235**, 146–159.

Xu, X., Zhao, B., Sun, M., Chen, X., Zhang, M., Li, H. & Xu, S. 2017 Co-pyrolysis characteristics of municipal sewage sludge and hazelnut shell by TG-DTG-MS and residue analysis. *Waste Management* **62**, 91–100.

Yi, Z. J., Yao, J., Wang, F., Chen, H. L., Liu, H. J. & Yu, C. 2013 Removal of uranium(VI) from aqueous solution by apricot shell activated carbon. *Journal of Radioanalytical and Nuclear Chemistry* **295** (3), 2029–2034.

Yuşan, S. 2017 U(VI) iyonlarının ham ve modifiye edilmiş diyatomit üzerine adsorpsiyon özelliklerinin kinetik ve termodinamik olarak incelenmesi. *Celal Bayar Üniversitesi Fen Bilimleri Dergisi* **13** (3), 761–768.

Zhu, C. S., Wang, L. P. & Chen, W. B. 2009 Removal of Cu (II) from aqueous solution by agricultural by-product: peanut hull. *Journal of Hazardous Materials* **168**, 739–746.

First received 10 March 2020; accepted in revised form 6 August 2020. Available online 18 August 2020